



Understanding the catalytic conversion of automobile exhaust emissions using model catalysts: CO + NO reaction on Pd(111)

E. Ozensoy,¹ C. Hess² and D.W. Goodman^{1*}

¹Department of Chemistry, Texas A&M University, P.O. Box 30012, College Station, TX 77842-3012

²Current address: Department of Inorganic Chemistry, Fritz-Haber-Institute of the MPG, Faradayweg 4-6, 14195 Berlin, Germany

* Corresponding author: e-mail goodman@mail.chem.tamu.edu

Abstract

The CO + NO reaction is one of the profoundly important reactions that take place on Pd-based industrial three-way catalysts (TWC). In this review, we discuss results from polarization modulation infrared reflection absorption spectroscopy (PM-IRAS) and conventional IRAS experiments on CO adsorption, NO adsorption and the CO + NO reaction on a Pd(111) model catalyst surface within a wide range of pressures (10^{-6} - 450 Torr) and temperatures (80 - 650 K). It will be shown that these studies allow for a detailed understanding of the adsorption behavior of these species as well as the nature of the products that are formed during their reaction under realistic catalytic conditions. CO adsorption experiments on Pd(111) at elevated pressures reveal that CO overlayers exhibit similar adsorption structures as found for ultrahigh vacuum (UHV) conditions. On the other hand, in the case of the CO + NO reaction on Pd(111), the pressure dependent formation of isocyanate was observed. The importance of this observation and its effects on the improvement of the catalytic NO_x abatement is discussed. The kinetics of the CO + NO reaction on Pd(111) were also investigated and the factors affecting its selectivity are addressed.

Keywords: Pd, CO, NO, NO_x, infrared, TWC, Pd(111), isocyanate, -NCO

1. Introduction

In the last few decades, the constant increase in the number of environmental protection regulations world wide has brought about significant restrictions on the nature and the quantity of the exhaust gases originating from mobile sources such as automobile emissions. These increasingly demanding criteria for exhaust emissions led to an intense scientific interest in the development of catalytic converters with higher performance and longer lasting stability. Pt/Rh (90/10) three way catalysts (TWC) that simultaneously oxidize CO to CO₂, reduce NO_x to N₂ and combust unburned hydrocarbons [1] were developed in 1970's as an initial solution for this technological problem. In the mid-1990's, Pd-only TWCs consisting of Pd particles deposited on a high surface area metal-oxide support (typically γ -Al₂O₃) containing varying amounts of stabilizers and/or promoters such as CeO₂, SiO₂, La₂O₃, and BaO were

introduced as an alternative to Pt/Rh (90/10) catalyst. Pd rapidly became the most highly consumed precious metal by the automobile industry for emission control purposes due to its technical and economical advantages [2].

A detailed understanding of the fundamental chemical and physical phenomena that take place on the active sites of the catalysts as well as on the catalyst supports at the molecular level is crucial in order to design heterogeneous catalysts with higher performance. Therefore, properties of the Pd based model heterogeneous catalyst systems for gas/solid interfaces have been investigated extensively in our laboratories [3-51]. Particularly, Pd single crystal surfaces [3],[4-21] Pd/X bimetallic systems (X= Mo [22-25], Ru [26-29], Cu [28;30], Ta [25;29;31], W [25;29;32;33], Re [25-27;29]), Pd/X/Y trimetallic systems (X/Y= Cu/Mo [34], Au/Mo [34]), Pd clusters deposited on SiO₂ [10;35-41], Al₂O₃ [42-47], TiO₂ [48-51] and MgO

[49;51] have been examined using various surface spectroscopic tools.

Surface specific vibrational spectroscopic techniques are exceptionally well-suited tools for elucidating heterogeneous catalytic reaction mechanisms as they provide unique possibilities to identify active species on the catalyst surface with sub-monolayer accuracy and enable an *in situ* analysis of catalysts under reaction conditions, in real time. In this respect, infrared reflection absorption spectroscopy (IRAS) [7;9;52-54], polarization modulation infrared reflection absorption spectroscopy (PM-IRAS) [17;20;21;39;55], high resolution electron energy loss spec-

troscopy (HREELS) [56-60], sum frequency generation (SFG) [61], and derivatives of these techniques [62] have been frequently used. In the current report, we discuss our vibrational spectroscopic results regarding the CO and NO adsorption as well as the mechanism and kinetics of the CO + NO reaction on Pd-based model catalysts, which have been extended to elevated pressure conditions only recently using *in situ* PM-IRAS [17;20;21;55]. The adsorption of CO [63],[19;52;64-70] NO [56-58;71-87] as well as the CO + NO reaction [21;88-109] on Pd-based catalysts have been thoroughly investigated by other groups also, both experimentally and theoretically [110-121].

PM-IRAS Optics and Signal Processing

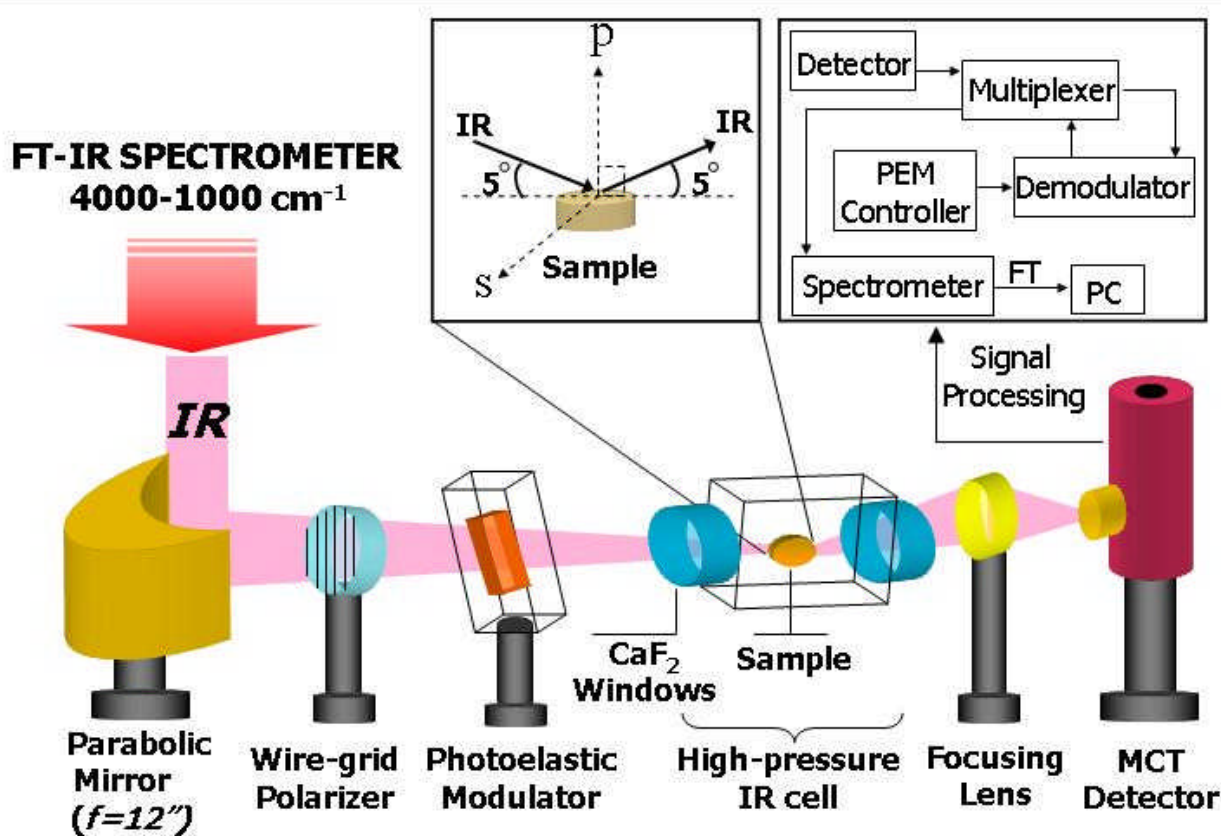


Figure 1. Schematic depicting the optical and electronic components of the PM-IRAS experimental setup.

The outline of this report is as follows: section 2 briefly describes the experimental techniques that are utilized in our studies. Basically, our approach to obtain a fundamental understanding of the complex surface phenomena is to start with simple but atomically well-defined model systems that can be studied with high experimental accuracy. We then increase the complexity of the examined model catalyst system in a controlled manner to mimic crucial aspects of a realistic/working heterogeneous catalyst. Therefore, section 3 starts with the investigation of the adsorption behavior of each of the reactants of the CO + NO reaction on the atomically flat Pd(111) single crystal surface, both under UHV and elevated pressure conditions (~450

Torr) using PM-IRAS and conventional IRAS, respectively. As has been demonstrated previously in our group, Pd particles supported by SiO₂ [37] and Al₂O₃ [42] ultra-thin films exhibit mostly <111> facets (with a minor contribution from <100> facets). Therefore, in the present discussion, we will mostly focus on results obtained for the Pd(111) single crystal surface. Next, our IRAS results on the CO + NO co-adsorption and reaction on Pd(111) model catalysts under low pressure conditions (typically ~1 x 10⁻⁶ Torr) are discussed. Results of these initial low-pressure studies were also compared with the analogous experiments at elevated pressure conditions (~180 Torr), where isocyanate formation is observed. In addition, dependence of the isocyanate formation

on the total reactant pressure during the CO + NO reaction on Pd(111) is discussed and the implications of this observation on the catalytic NO_x removal are also addressed.

2. Experimental

The surface analysis chambers that have been utilized are UHV chambers coupled to a micro-reactor for *in situ* vibrational spectroscopic and kinetic studies. They include standard surface science techniques such as infrared reflection absorption spectroscopy (IRAS), polarization modulation infrared reflection absorption spectroscopy (PM-IRAS), Auger electron spectroscopy (AES), low energy electron diffraction (LEED) and temperature programmed desorption (TPD) spectroscopy. Pd single crystals were cleaned by performing repeated cycles of low temperature oxidation and subsequent high temperature annealing until the surfaces were found to be free of carbon, oxygen and sulfur contaminations as measured by AES.

PM-IRAS is a very versatile and a powerful *in situ* vibrational spectroscopic technique which can be applied to analyze surface properties of gas/solid interfaces at pressures close to atmospheric pressures with virtually no contribution from the gas phase species [17;20;21;39]. Briefly, the PM-IRAS setup used in this study consists of an infrared spectrometer (Bruker Equinox 55), a static wire-grid polarizer and a photoelastic modulator (PEM, Hinds instruments) to create a fast modulation of the polarization state of the incident light (ideally between s and p states). A demodulator-multiplexer electronics (GWC instruments, Bruker) is used to compute a differential reflectivity spectrum from the sum (p + s) and difference (p - s) signals collected by the mercury cadmium telluride (MCT) detector (fig. 1). For the NO adsorption and CO + NO experiments described below the PEM controller was set to 1700 cm⁻¹, whereas it was set to 1800 cm⁻¹ for the CO adsorption experiments. Data acquisition time for each of the PM-IRA spectra presented here was 4.5 min/spectra with a spectral resolution of 4 cm⁻¹ for the CO/Pd(111) experiments and 8 cm⁻¹ for the NO/Pd(111) and CO + NO/Pd(111) experiments.

CO, O₂, CO₂ and N₂O gases used in the experiments were of 99.99% purity or better, and the NO gas was C.P. grade. For the isotope experiments ¹³CO (99%) and ¹⁵NO (99%) were used. For CO adsorption experiments, CO was further purified using liquid nitrogen cold traps. This method allows the cleaning of CO up to 600 mbar, the vapor pressure of CO at 90 K. Purification of CO for pressures greater than 600 mbar was carried out using a n-pentane/liquid nitrogen slurry maintained at 143 K. Similarly, for NO adsorption and CO + NO reaction experiments, CO and NO gases were also purified using a n-pentane/liquid nitrogen slurry. To avoid any photo-induced NO₂ formation in the CO + NO gas mixture, both the pre-mixing/cleaning procedures and the experiments were conducted with the exclusion of visible light.

The CO + NO reaction was performed in batch mode and the product formation was followed with infrared spectroscopy by monitoring both the adsorption behavior on the Pd surface (via PM-IRAS) and the evolution of the gas

phase CO₂ and N₂O. The gas phase production of CO₂ and N₂O was calculated by converting infrared intensities into pressures by using a set of calibration curves. Turnover frequencies (TOF) were obtained by normalizing the gas phase production per second to the total number of surface sites.

For further experimental details, the reader is referred to our previous reports [7-10;13;17;20;21].

3. Results and Discussion

3.1. CO Adsorption on Pd(111)

Coverage-dependent ordered overlayers of CO on Pd(111) single crystal surfaces have been studied extensively in the literature [7;52;63;65]. Vibrational spectroscopy, in particular the C-O stretching frequency of adsorbed CO can be used for adsorption site assignments of these ordered CO layers by comparing these values with the inorganic metal-carbonyl analogues where the coordination of CO to the metal center is accurately known. Although this approach was criticized as misleading in some specific cases [63;73;122], it is found to be very useful for many other systems where site assignments via vibrational spectroscopy can be verified with other complementary methods [52;65;123].

At a CO coverage of $\theta_{\text{CO}} = 0.33$ ML (ML = monolayer), recent STM studies suggest that CO on Pd(111) forms overlayers with a ($\sqrt{3} \times \sqrt{3}$) R 30° - 1CO structure [65], occupying primarily 3-fold hollow adsorption sites (fig. 2). Using a combination of LEED and IRAS techniques it was previously demonstrated that this CO overlayer yields a distinctly low C-O vibrational frequency of ~1850 cm⁻¹ (fig. 3a) [52]. [7] As the CO coverage is further increased to $\theta_{\text{CO}} = 0.50$ ML, the adsorbed CO molecules exhibit two coexisting c(4x2)-2 CO or NO phases (fig. 2), where CO occupies

CO/Pd(111) and NO/Pd(111) ordered overlayer structures

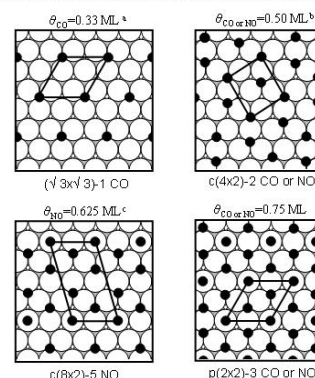


Figure 2. Structures of the ordered overlayers that are formed during NO or CO adsorption on the Pd(111) single crystal surface (see text for details). ^a This structure is only observed for CO. NO forms a disordered phase at $\theta_{\text{NO}} = 0.33$ ML [124]. ^b A similar phase with bridging adsorption was also proposed for CO/Pd(111) at $\theta_{\text{CO}} = 0.33$ ML. ^c Complex overlayer structures were reported for CO/Pd(111) at this coverage where mostly bridging sites are occupied [65].

either the bridging sites or 3-fold hollow sites [65]. These structures correspond to a C-O vibrational frequency of $\sim 1920\text{ cm}^{-1}$ [7;52]. Within $\theta_{\text{CO}} = 0.50 - 0.75\text{ ML}$, various complex overlayer structures have been reported [65], which result in a CO vibrational band near 1965 cm^{-1} [52]. Recent STM experiments combined with density functional theory (DFT) calculations suggest that CO occupies primarily bridging sites on the Pd(111) surface within this coverage regime [65]. Eventually, at $\theta_{\text{CO}} = 0.75\text{ ML}$, the CO saturation coverage is obtained yielding a (2x2) - 3CO structure (fig. 2). Within this structure, CO resides on both atop and 3-fold hollow sites corresponding to vibrational bands at 2110 and 1895 cm^{-1} , respectively (fig. 3a) [7;52]. These adsorption site assignments for the CO/Pd(111) system at low pressures ($\sim 1 \times 10^{-8}\text{ Torr}$) have been confirmed by the combined STM and DFT studies of Rose and coworkers [65].

The adsorption of CO on Pd(111) was also investigated at elevated pressures using PM-IRAS [20]. In this recent study (see fig. 3b) [20] it was demonstrated that CO overlayers follow similar trends in terms of the observed vibrational frequencies within $10^{-6} - 450\text{ Torr}$ (i.e. within a

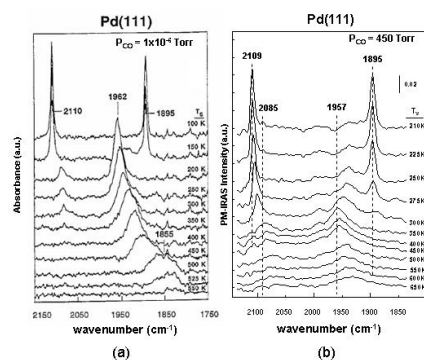


Figure 3. In situ IR spectra for CO adsorption on Pd(111) at $P_{\text{CO}} = 1 \times 10^{-6}\text{ Torr}$ (a) [7] and in situ PM-IRAS spectra for CO adsorption on Pd(111) at $P_{\text{CO}} = 450\text{ Torr}$ (b) [20]. All of the spectra are acquired *in the presence of the CO gas phase*. Initial adsorption was performed at the highest temperature given in each of the spectral series.

dynamic pressure range of nine orders of magnitude!), implying that no new pressure-induced species nor adsorbate-induced surface reconstructions occur on the Pd(111) surface during CO adsorption at elevated pressures. Therefore, an equilibrium phase diagram was constructed showing the different types of Pd(111) sites that are occupied by adsorbed CO molecules at various pressure and temperature regimes (fig. 4). Furthermore, a transition from a phase dominated by CO molecules adsorbed on bridging sites to a different phase where CO resides on atop/3-fold hollow sites is monitored by varying the CO pressure within 9 orders of magnitude. The apparent activation energy of this phase transition was calculated to be 44.3 kJ/mol (fig. 4) [20].

Equilibrium (Bridging - 3-fold/atop) Phase Transition Diagram for CO / Pd(111)

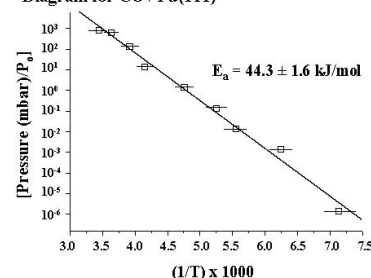


Figure 4. Isosteric plot for the phase transition from bridging to atop/threefold CO on Pd(111).

The elevated pressure PM-IRAS results for the CO adsorption on the Pd(111) single crystal model catalyst discussed above provide important insights about the correlation between traditional surface science studies performed under UHV/low-temperature conditions and the real heterogeneous catalytic applications where elevated pressures and temperatures are employed. Our PM-IRAS results on CO adsorption on Pd(111) clearly indicate that UHV studies can be readily extrapolated to estimate the state of the examined catalytic system under more realistic conditions. These findings also demonstrate the wide-ranging experimental *in situ* capabilities offered by PM-IRAS which make it a powerful, yet experimentally straight forward technique that can be successfully applied to bridge the so-called *pressure gap* between surface science and heterogeneous catalysis.

3.2. NO Adsorption on Pd(111)

In terms of their coverage dependent ordered structures, NO overlayers on Pd(111) show striking similarities to the CO overlayers on Pd(111) (see fig. 2) [8;55;56;58;73;75;84;106;124]. In the literature, a $c(4 \times 2)$ phase at $\theta_{\text{NO}} = 0.5\text{ ML}$ [8;58;75;124], which transforms into an ordered phase with a $c(8 \times 2)$ structure at $\theta_{\text{NO}} = 0.625\text{ ML}$ [8] was reported, in addition to the $p(2 \times 2)$ overlayer at the NO saturation coverage of $\theta_{\text{NO}} = 0.75\text{ ML}$ [8;58;75]. Besides these ordered structures, another overlayer structure, which lacks long range order, was also reported for low NO coverages ($\theta_{\text{NO}} = 0.33\text{ ML}$) [58;75;124]. It should be noted that there has been a long-standing controversy regarding the adsorption site assignments for these NO overlayers using vibrational spectroscopic techniques [73]. For instance, the adsorption sites for the $c(4 \times 2)$ structure that was originally associated with the bridging sites [8;58;75] were assigned to atop sites in a later study [106]. On the other hand, DFT studies proposed that NO occupies 3-fold hollow [117] or 3-fold hollow + atop [76] sites in this phase.

A recent report by Hansen and coworkers [76], which combines atomic resolution STM and DFT calculation studies seems to resolve this long-standing controversy. By employing these two powerful methods, the authors suggest that NO molecules reside on the 3-fold hollow (fcc and

hcp) sites in the $c(4 \times 2)$ -2NO domains (fig. 2). In the $c(8 \times 2)$ -5NO domains, each NO overlayer unit cell consists of four NO molecules occupying fcc and hcp 3-fold sites in addition to one NO molecule on the atop sites (fig. 2). It was also argued in the same study that NO molecules on the atop sites are tilted with respect to the surface normal in the $c(8 \times 2)$ -5NO phase. For the $p(2 \times 2)$ -3NO domains, they propose a unit cell structure where one NO molecule occupies atop sites with a tilted orientation with two other NO molecules sitting on the 3-fold hollow sites (fcc and hcp). Another important observation regarding the NO/Pd(111) adsorption system in this report is the simultaneous coexistence of different ordered NO overlayers on the Pd(111) surface. STM results [76] reveal that at a coverage regime where a complete $c(8 \times 2)$ -5NO overlayer is expected, NO

molecules on Pd(111) *always* exist as separate coexisting domains of $c(8 \times 2)$ -5NO, $c(4 \times 2)$ -2NO and $p(2 \times 2)$ -3NO. This observation was explained using the adsorption energetics of the different NO overlayers. Due to the repulsive interaction between the adsorbed NO molecules on Pd(111), the NO chemisorption potential energy is found to be monotonically decreasing with increasing coverage [76]. In other words, the NO chemisorption potential for the $p(2 \times 2)$ -3NO phase is lower than for the $c(8 \times 2)$ -5NO phase, whereas the NO chemisorption potential for $c(4 \times 2)$ -2NO is higher than that of the $c(8 \times 2)$ -5NO domains. Thus the total energy of the NO/Pd(111) system with a complete $c(8 \times 2)$ -5NO overlayer can also be reached by having separate domains of $c(8 \times 2)$ -5NO, $c(4 \times 2)$ -2NO and $p(2 \times 2)$ -3NO overlayers existing simultaneously.

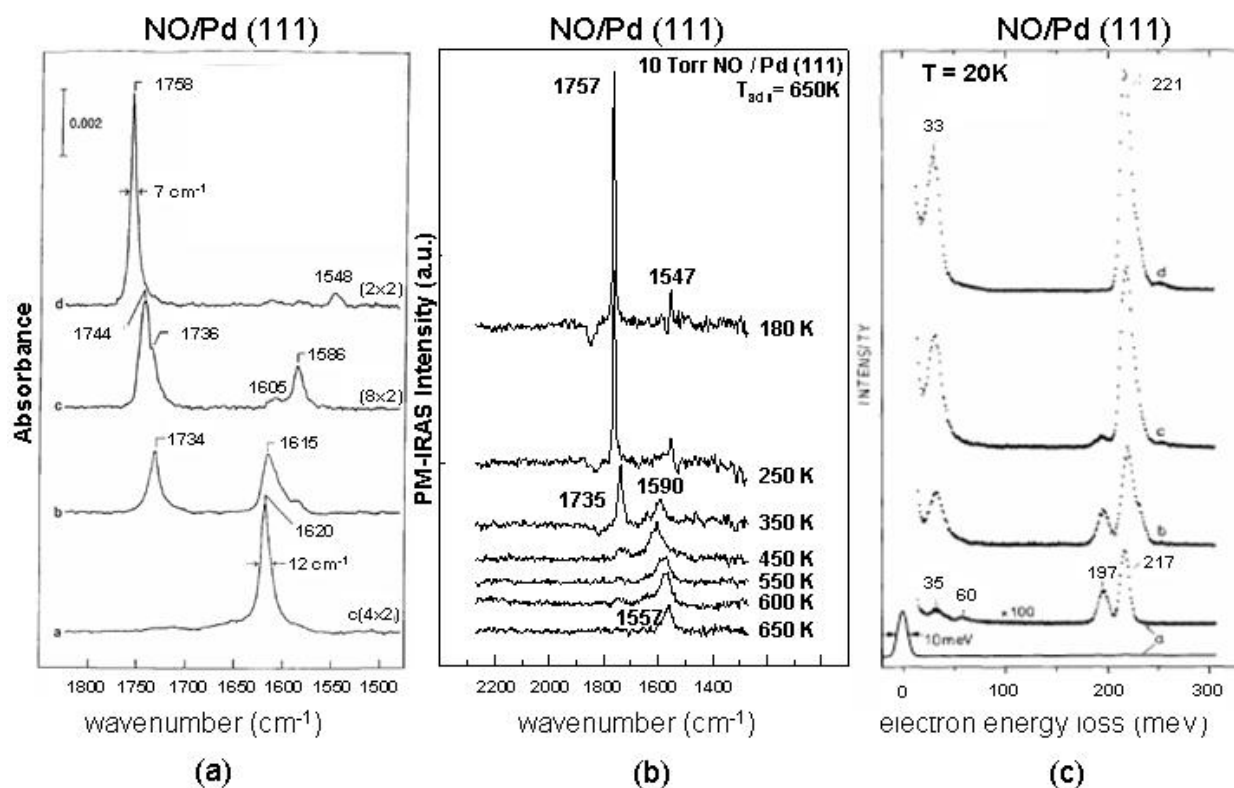


Figure 5. (a) IRAS data representative of the ordered overlayers of NO on Pd(111) obtained at $P_{\text{NO}} \sim 10^{-6}$ Torr [8]. (b) PM-IRA spectra for NO adsorption on Pd(111) at 10 Torr [55]. (c) HREEL spectra for low temperature (20 K) NO adsorption on Pd(111) with increasing NO coverage and NO-dimer formation [58].

Vibrational spectroscopic results [8;55;58] for NO/Pd(111) can be interpreted more accurately in the light of the information provided by these recent STM and DFT studies [76]. Fig. 5a [8] shows the IRAS results obtained for the NO/Pd(111) system at low pressures ($P_{\text{NO}} \sim 1 \times 10^{-6}$ Torr). At a NO coverage of $\theta_{\text{NO}} = 0.5$ ML, a LEED pattern corresponding to a $c(4 \times 2)$ -2NO structure is obtained. At the same coverage a N-O stretching band at 1620 cm^{-1} is observed. Based on the arguments given above, this adsorption band can be assigned to NO molecules residing on 3-fold

hollow sites. As the NO coverage is increased, a red shift in the NO band (corresponding to 3-fold hollow sites) to 1615 cm^{-1} is observed. In addition, another high frequency adsorption band around 1734 cm^{-1} appears that can be attributed to NO bound to atop sites. When a NO coverage of $\theta_{\text{NO}} = 0.625$ ML is reached, a LEED pattern suggesting a $c(8 \times 2)$ -5NO phase is obtained. NO bands at 1744 and 1736 cm^{-1} are observed corresponding to NO species at different atop adsorption sites. Two other low frequency bands at ~ 1605 and 1586 cm^{-1} correspond to adsorption on 3-fold

As the previous STM studies suggest that the $c(8 \times 2)$ -5NO phase always coexists with the $c(4 \times 2)$ -2NO and $p(2 \times 2)$ -3NO domains [76], the IRA spectrum for the (8×2) phase should indeed be a convolution of all these three separate domains. This argument provides a new interpretation for the spectrum in fig. 5a, suggesting that the shoulder at $\sim 1605 \text{ cm}^{-1}$ can be associated with the NO molecules sitting on the 3-fold hollow sites of $c(4 \times 2)$ -2NO domains. Similarly the high frequency adsorption band at 1744 cm^{-1} can be attributed to NO species occupying atop sites of $p(2 \times 2)$ -3NO domains. Then the remaining two features at 1736 and 1586 cm^{-1} can be readily assigned to NO species adsorbed on atop and 3-fold hollow sites of $c(8 \times 2)$ -5NO domains, respectively.

At a saturation coverage of $\theta_{\text{NO}} = 0.75 \text{ ML}$, a $p(2 \times 2)$ -3NO overlayer structure is formed as confirmed by the LEED images [8] and the IRAS data that yield two distinct NO adsorption bands at 1758 cm^{-1} and 1548 cm^{-1} due to atop and 3-fold hollow adsorption, respectively. An interesting aspect of the topmost IRA spectrum in fig. 5a is the relative IR intensity of the NO species corresponding to atop and 3-fold hollow sites. As the $p(2 \times 2)$ -3NO unit cell structure implies the presence of two NO molecules adsorbed on hollow sites for every NO molecule sitting on the atop sites, the smaller IRAS intensity for the NO molecules residing on the hollow sites with respect to the atop sites suggests that the IRAS cross sections for these two adsorbed states should be considerably different. This well known effect is demonstrated in a recent DFT study [125] where it was shown that the IR cross sections for CO molecules on atop and hollow sites of Pd(111) may vary by a factor of four as a function of the coverage-dependent overlayer structure. Fig. 5b shows the PM-IRAS results [55] for NO adsorption on Pd(111) at elevated pressures ($P_{\text{NO}} = 10 \text{ Torr}$). It is clearly seen that the vibrational adsorption bands for NO follow similar trends from 10^{-6} up to 10 Torr . Further details of the elevated pressure experiments on the NO/Pd(111) adsorption system will be discussed in a forthcoming publication [55].

It has been demonstrated previously that at lower adsorption temperatures such as 20 K , in addition to the previously mentioned NO species, a new NO adsorption band at 1782 cm^{-1} (221 meV) is observed on Pd(111) using HREELS [124], which displays a shoulder at $\sim 1860 \text{ cm}^{-1}$ (230 meV) (fig. 5c). These two low-temperature NO bands (221 and 230 meV) were attributed to the asymmetric and symmetric stretching modes of a weakly bound NO-dimer species ($(\text{NO})_2$), respectively. The formation of a similar weakly bound NO-dimer species has also been observed in recent PM-IRAS studies on the NO/Pd(111) adsorption system at elevated pressures [55]. Observation of $(\text{NO})_2$ species on Pd(111) deserves special attention as it has been shown in the literature that N_2O is formed on Ag(111) via an $(\text{NO})_2$ intermediate [73].

The dissociation of NO on Pd(111) at high temperatures ($373 - 518 \text{ K}$) has also been investigated by HREELS [56] and TPD [13;56] under UHV conditions. HREELS studies reveal that NO desorbs mostly molecularly from the Pd(111) surface around 500 K with a small amount of dissociation above 490 K [56]. However, it was reported

that NO dissociation is significantly facilitated in the presence of surface steps such as in the case of the stepped Pd(112) surface [56]. In case of Pd(111), atomic O species formed (due to NO dissociation) are detected only up to 550 K [56]. Above this temperature, atomic O is reported to dissolve into the bulk to form subsurface O. No O_2 was detected in TPD studies of NO desorption from a Pd(111) surface although other dissociation products such as NO, N_2 and N_2O were readily observed [13;56].

3.3 CO + NO coadsorption and reaction on Pd(111)

3.3.1 CO + NO reaction on Pd(111) at low pressures

As discussed above, the CO/Pd(111) and NO/Pd(111) adsorption systems are now understood in great detail. In the following section, the more complex interaction of CO and NO during the CO + NO reaction on the Pd(111) model catalyst is addressed. Fig. 6 [13] presents

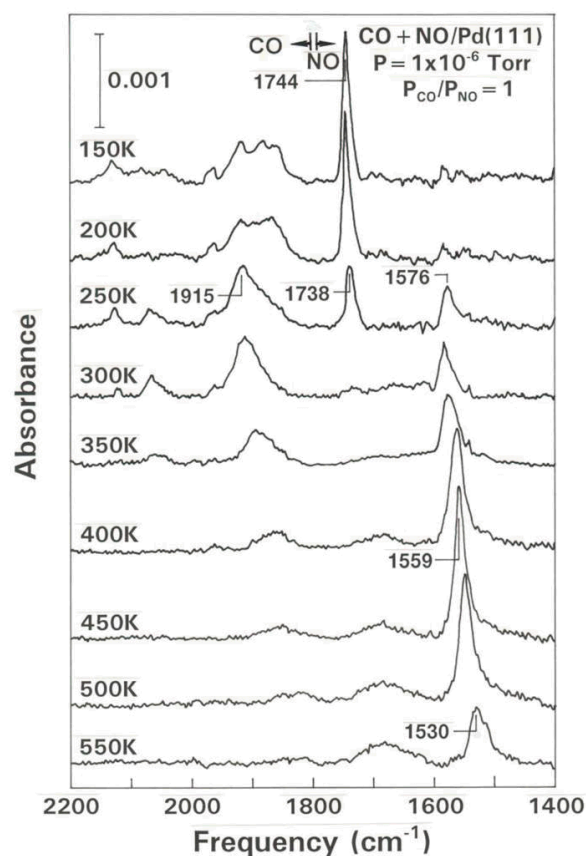


Figure 6. Low pressure IRA spectra for CO + NO coadsorption and reaction on Pd(111) where $P_{\text{CO+NO}} = 1 \times 10^{-6} \text{ Torr}$ and $P_{\text{CO}}/P_{\text{NO}} = 1$ [10].

temperature dependent IRAS results for CO + NO coadsorption on a Pd(111) single crystal model catalyst surface ($P_{\text{CO+NO}} = 1 \times 10^{-6} \text{ Torr}$, $P_{\text{CO}}/P_{\text{NO}} = 1$). The series of spectra in fig. 6 reveals that CO occupies predominantly 3-fold hollow sites ($\sim 1915 \text{ cm}^{-1}$) under both low and high temperature conditions, whereas NO prefers atop sites (1744 cm^{-1}) at low temperatures and 3-fold hollow sites ($1576 - 1530 \text{ cm}^{-1}$) at high temperatures [13]. In addition, at the saturation coverage, NO and CO bands on Pd(111) have similar intensities,

whereas at lower coverages NO bands have a significantly higher intensity. This is consistent with recent theoretical calculations [113] suggesting that NO has a relatively higher adsorption energy at saturation coverage with respect to CO, whereas at low coverages these two adsorbates have similar adsorption energetics.

A comparative look at the IRAS data allows us to obtain important clues about the nature of the CO and NO adsorption on the transition metal surfaces. The Blyholder model [70] has been widely used to interpret the frequency shifts for CO adsorption bands in vibrational spectroscopic experiments. According to this model, CO binds to the metal surface via electron donation from its 5σ orbital that is accompanied by a backdonation from the metal $d\pi$ orbital to the empty $2\pi^*$ orbital of CO. As the CO coverage increases, depletion of the electron density of the metal d band results in a decreased back donation to the $2\pi^*$ orbital of CO which leads to a vibrational blue shift in the C-O stretching frequency. On the other hand, NO containing one more electron than CO in its $2\pi^*$ orbital, can form a covalent bond with the metal surface also through other models [126] such as spin pairing of the NO $2\pi^*$ electron with a metal $d\pi$ electron to form a covalent π bond. This is accompanied by electron donation from the NO 5σ orbital to an empty σ orbital of the metal to obtain a linear geometry or spin pairing of the NO $2\pi^*$ electron with a metal σ electron to assume a tilted geometry. In the latter case, only little donation from the NO 5σ orbital to the metal occurs. IRAS experiments [127] on CO + NO coadsorption on Pd(111) at 300 K, from the minimum detectable coverages to the saturation coverages, indicate that the frequency shift for the CO adsorption bands is +77 whereas the corresponding shift for NO is only +46 cm^{-1} , respectively. This marked difference in the magnitude of the coverage dependent vibrational blue shifts of NO compared to CO may suggest that the backdonation from the metal d band to the NO $2\pi^*$ orbitals may not necessarily be the prominent factor for the nature of the Pd-NO bond. However, $5\sigma/2\pi^*$ donation from NO to Pd may have a larger contribution to the observed frequency shifts. Thus with increasing NO coverage, the smaller degree of 5σ donation from NO to the metal may have only a small effect on the strength of the N-O bond as the 5σ orbital is only slightly antibonding (contrary to the CO $2\pi^*$ orbital). Hence the smaller coverage dependence of the N-O stretching frequency on Pd surfaces can be explained by the stabilization of the Pd-NO bond as a result of the primarily covalent bonding interaction [126].

3.3.2 CO + NO reaction on Pd(111) at elevated pressures and the formation of isocyanate

Recently, the CO + NO reaction has also been studied at elevated pressures using in situ PM-IRAS [17;21]. Fig. 7 shows the PM-IRA spectra obtained in the presence of a total CO + NO pressure of 240 mbar (i.e. 180 Torr) with $P_{\text{CO}}/P_{\text{NO}} = 1.5$. Comparison of low (fig. 6) and high pressure (fig. 7) results for the CO + NO reaction on Pd(111) suggests that NO and CO occupy similar adsorption sites in both pressure regimes.

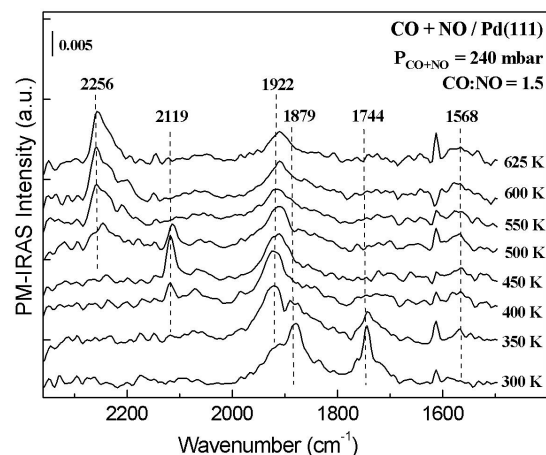


Figure 7. In situ PM-IRA spectra for CO + NO coadsorption and reaction on Pd(111) at 240 mbar (180 Torr), $P_{\text{CO}}/P_{\text{NO}} = 1.5$ [21].

Furthermore, CO_2 yields determined by gas phase IR spectroscopy (fig. 8) suggest that the reaction rate is insignificant below 550 K. However, above this

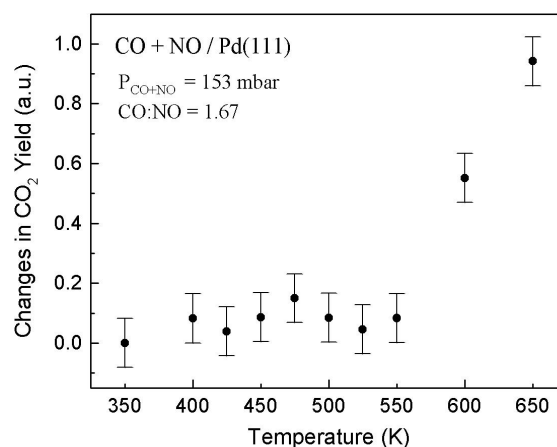


Figure 8. Relative CO_2 conversion versus temperature in CO + NO reaction on Pd(111) (each data point represented here was obtained by integrating CO_2 yield for a period of 5 minutes at each given temperature) [21].

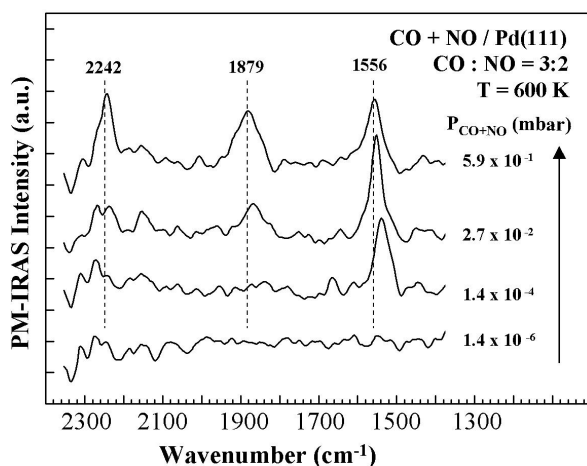
temperature, a drastic increase in the reaction rate is observed. Besides the anticipated CO and NO adsorption bands in fig. 7, above 500 K, the development of another feature at 2256 cm^{-1} is also visible. Isotopic labeling experiments revealed that this feature is associated with an isocyanate ($-\text{NCO}$) species that is formed during the reaction between adsorbed CO and atomic N, which is formed via dissociation of NO on Pd(111) (Table 1) [17]. $-\text{NCO}$ formation in the CO + NO reaction on Pd catalysts have also been reported in the literature, both in experimental [89;90;128-132] and theoretical [95] studies. It has been suggested that $-\text{NCO}$ is formed on the metal centers and then spills over to the oxide support [133]. Along these lines, Solymosi and coworkers [133] reported that the vibrational features for $-\text{NCO}$ species on supported metal particles strongly depend on the nature of the oxide but not on the type of the metal.

TABLE 1. Comparison of the isocyanate group frequencies and isotope frequency shifts (in cm^{-1}) on Pd(111) and Cu(100).

	$^{14}\text{N}^{12}\text{CO}$	$^{14}\text{N}^{13}\text{CO}$	$^{15}\text{N}^{12}\text{CO}$	$^{13}\text{CO}-^{12}\text{CO}$	$^{15}\text{NO}-^{14}\text{NO}$
Cu(100) ^a	2198	2140	2192	-58	-6
Pd(111) ^b	2243	2178	2230	-65	-13

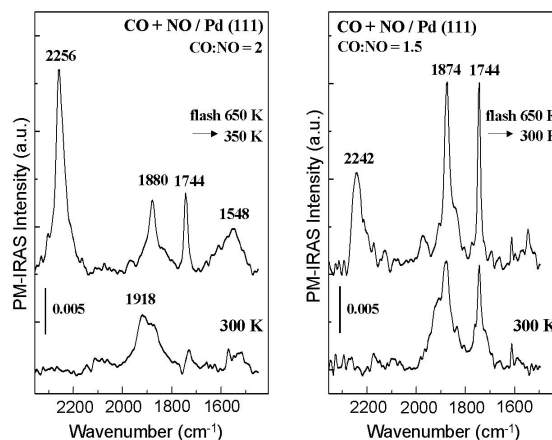
^aCelio et al. [134].^bOzensoy et al. [17]. For the CO + NO and CO + ^{15}N mixtures $P_{\text{total}} = 0.67$ mbar ($\text{CO}/^{14,15}\text{NO} = 1.5$), for the ^{13}CO + NO mixture $P_{\text{total}} = 1.06$ mbar ($^{13}\text{CO}/\text{NO} = 1.3$). Mixtures were dosed at 600 K.

As the $-\text{NCO}$ formation mechanism on Pd(111) implies NO dissociation, formation of isocyanate can be used as a sensitive indicator for the NO dissociation process, which is a crucial step in the CO + NO reaction. Detection of $-\text{NCO}$ at 500 K (see fig. 7), where the CO + NO reaction is still relatively slow, suggests that NO dissociation may not be the limiting step at this temperature. A very interesting aspect of isocyanate formation on Pd(111) at elevated pressures was demonstrated by varying the total pressure of the CO + NO gas phase (fig. 9) [17]. It was shown that isocyanate formation is *only* detected at elevated pressures

**Figure 9.** PM-IRAS data illustrating the pressure dependent formation of isocyanate ($-\text{NCO}$) during CO + NO reaction on Pd(111) [17].

(above 0.02 mbar) emphasizing the profound significance of in situ investigations of heterogeneous catalytic reactions under realistic experimental conditions. Furthermore, dependence of the $-\text{NCO}$ formation on the relative ratio of the partial pressures of the reactants in CO+NO reaction was also examined. Fig. 10 [21] shows that $-\text{NCO}$ formation is significantly enhanced when the partial pressure of CO is increased in the reactant mixture. Besides, $-\text{NCO}$ was found to be extremely stable on Pd(111). Once it is formed at $T > 500$ K it was found to be stable within 300-650 K and

even after pumping out the reactant gases down to $\sim 10^{-7}$ Torr at 300 K. These results are in contrast to the Rh(111) case where it was found that $-\text{NCO}$ has a very short lifetime and decomposes to N_2 and CO even at room temperature in the absence of an oxide support [133].

**Figure 10.** Influence of $P_{\text{CO}}/P_{\text{NO}}$ partial pressure ratio on the amount of isocyanate formed on Pd(111) surface during CO + NO reaction [21].

The interesting chemistry of $-\text{NCO}$ in the CO + NO reaction on platinum group metals deserves special attention as it was suggested that $-\text{NCO}$ intermediate may provide important practical improvements in the catalytic NO_x abatement. Unland et al. proposed that in the presence of H_2O , NH_3 can also form during the CO + NO reaction on supported Pd catalysts via hydrolysis of an $-\text{NCO}$ intermediate [128;129]. Recently, Lambert et al. studied CO + NO + H_2 + O_2 and CO + NO + H_2O reactions on a Pd/ Al_2O_3 supported catalyst and showed the formation of NH_3 via hydrolysis of an $-\text{NCO}$ intermediate [130]. They suggested that NH_3 formation during these reactions may provide an additional route for NO_x removal as it eliminates the necessity for the addition of an external reducing agent such as NH_3 . It was argued in the same study [130] that the performance of the H_2 + O_2 + CO + NO reactant mixture is superior to the H_2O +CO+NO mixture towards NH_3 forma-

tion on a high surface area Pd/Al₂O₃ catalysts. It was suggested that although NH₃ formation takes place through the hydrolysis of -NCO in both cases, H₂ adsorption on Pd particles may further weaken the N-O bond on Pd sites and thus enhance the NO dissociation and subsequent -NCO formation process. It should be also mentioned that in the presence of H₂, NH₃ formation can also readily occur via an alternative pathway which is the hydrogenation of atomic N. In a related study, Cant and coworkers [131] [132] demonstrated the formation of gas phase HNCO in the CO + NO + H₂ reaction on high surface area Pd/SiO₂ and Pt/SiO₂ catalysts. This interesting finding supported the possibility that hydrolysis of -NCO to form NH₃ can take place via an HNCO intermediate as originally proposed by Unland et al. [128]. Consequently, although -NCO seems to be a spectator in CO+NO reaction on Pd (111), in the presence of hydrogen containing species such as H₂ or H₂O, -NCO acts as an important intermediate on high surface area Pd catalysts to produce an additional reducing agent (NH₃) that can further enhance catalytic NO_x removal.

The temperature dependent selectivity of the CO + NO reaction on Pd(111) was also investigated at elevated pressures (fig. 11) [21]. Some of the important factors which lead to the observed temperature dependence of N₂O selectivity can be explained by considering the branching ratio between the two major reaction pathways that have been suggested previously for the CO + NO reaction on Pd(111) [13;14;14;44]:

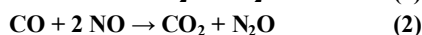
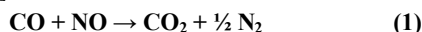


Fig. 11 illustrates that the N₂O selectivity monotonically increases with increasing temperature in the reac-

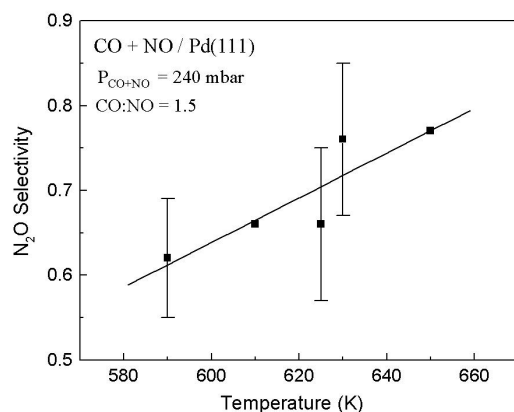


Figure 11. N₂O selectivities, N₂O/(N₂ + N₂O), for the CO + NO reaction on Pd(111) at 240 mbar total pressure (P_{CO}/P_{NO} = 1.5) [21].

tion regime (i.e. within 590-660 K). By looking at the series of spectra in figs. 6 and 7, it can be realized that the relative

concentrations of adsorbed NO to CO on the Pd(111) surface ([NO]_{ads}/[CO]_{ads}) also increase with increasing temperature in this temperature interval. As increasing [NO]_{ads}/[CO]_{ads} forces pathway (2) to dominate, the N₂O selectivity increases with increasing temperature under reaction conditions.

4. Conclusions

In this report we have addressed the CO adsorption, NO adsorption and CO + NO reaction on a Pd(111) single crystal model catalyst surface by discussing results from vibrational spectroscopic experiments obtained within a wide range of pressures and temperatures. In the case of the CO/Pd(111) adsorption system, we have demonstrated that the results of traditional surface scientific experiments under UHV conditions can be accurately extrapolated to the high-temperature/high pressure regime even if the pressure differential between these two cases may be as large as 10⁹. It was shown that similar coverage dependent CO overlayer structures are observed on Pd(111) without any indication for new pressure-induced species or occurrence of adsorbate-induced surface reconstructions at elevated pressures. On the other hand, by employing *in situ* PM-IRAS to study the CO + NO reaction on Pd(111) at elevated pressures, we demonstrated the formation of -NCO and discussed some of the important implications of this observation regarding catalytic NO_x removal. These striking experimental results obtained by utilizing the powerful *in situ* capabilities of the PM-IRAS technique clearly emphasize the significance of studying heterogeneous catalytic reactions under realistic conditions such as elevated pressures and temperatures.

Acknowledgments

We acknowledge with pleasure the support of this work by the Department of Energy, Office of Basic Energy Sciences, Division of Chemical Sciences, and the R. A. Welch Foundation and the Texas Advanced Technology Program under Grant No. 010366-0022-2001. The authors would like to acknowledge R. M. Lambert and N.W. Cant for fruitful discussions. C. H. thanks the Alexander von Humboldt foundation for providing a Feodor Lynen fellowship.

References

- [1] R. M. Heck and R. J. Farrauto. Catalytic Air Pollution Control: Commercial Technology. 1995. New York, NY, International Thomson Publishing.
- [2] A. H. Tullio. Chemical & Engineering News 80[34], 17. 2002.
- [3] B. D. Kay, C. H. F. Peden, and D. W. Goodman, Physical Review B, 34 (1986) 817-821.
- [4] C. H. F. Peden, B. D. Kay, and D. W. Goodman, Surface Science, 175 (1986) 215-225.

- [5] P. J. Berlowitz and D. W. Goodman, *Journal of Catalysis*, 108 (1987) 364-368.
- [6] P. J. Berlowitz, C. H. F. Peden, and D. W. Goodman, *Journal of Physical Chemistry*, 92 (1988) 5213-5221.
- [7] W. K. Kuhn, J. Szanyi, and D. W. Goodman, *Surface Science*, 274 (1992) L611-L618.
- [8] P. J. Chen and D. W. Goodman, *Surface Science*, 297 (1993) L93-L99.
- [9] J. Szanyi, W. K. Kuhn, and D. W. Goodman, *Journal of Vacuum Science & Technology A-Vacuum Surfaces and Films*, 11 (1993) 1969-1974.
- [10] X. P. Xu, P. J. Chen, and D. W. Goodman, *Journal of Physical Chemistry*, 98 (1994) 9242-9246.
- [11] J. Szanyi, W. K. Kuhn, and D. W. Goodman, *Journal of Physical Chemistry*, 98 (1994) 2978-2981.
- [12] J. Szanyi and D. W. Goodman, *Journal of Physical Chemistry*, 98 (1994) 2972-2977.
- [13] S. M. Vesecky, P. J. Chen, X. P. Xu, and D. W. Goodman, *Journal of Vacuum Science & Technology A-Vacuum Surfaces and Films*, 13 (1995) 1539-1543.
- [14] S. M. Vesecky, D. R. Rainer, and D. W. Goodman, *Journal of Vacuum Science & Technology A-Vacuum Surfaces and Films*, 14 (1996) 1457-1463.
- [15] D. W. Goodman, *Journal of Physical Chemistry*, 100 (1996) 13090-13102.
- [16] M. Bowker, R. P. Holroyd, R. G. Sharpe, J. S. Corneille, S. M. Francis, and D. W. Goodman, *Surface Science*, 370 (1997) 113-124.
- [17] E. Ozensoy, C. Hess, and D. W. Goodman, *Journal of the American Chemical Society*, 124 (2002) 8524-8525.
- [18] D. Meier, E. Ozensoy, and D. W. Goodman, to be submitted.
- [19] A. K. Santra and D. W. Goodman, *Electrochimica Acta*, 47 (2002) 3595-3609.
- [20] E. Ozensoy, D. C. Meier, and D. W. Goodman, *Journal of Physical Chemistry B*, 106 (2002) 9367-9371.
- [21] C. Hess, E. Ozensoy, and D. W. Goodman, *Journal of Physical Chemistry B*, 107 (2003) 2759-2764.
- [22] C. Xu and D. W. Goodman, *Langmuir*, 12 (1996) 1807-1816.
- [23] C. Xu and D. W. Goodman, *Journal of Physical Chemistry*, 100 (1996) 245-252.
- [24] C. Xu and D. W. Goodman, *Journal of Physical Chemistry B*, 102 (1998) 4392-4400.
- [25] J. A. Rodriguez and D. W. Goodman, *Journal of Physical Chemistry*, 95 (1991) 4196-4206.
- [26] J. A. Rodriguez, R. A. Campbell, and D. W. Goodman, *Surface Science*, 309 (1994) 377-383.
- [27] R. A. Campbell, J. A. Rodriguez, and D. W. Goodman, *Physical Review B*, 46 (1992) 7077-7087.
- [28] J. A. Rodriguez, R. A. Campbell, and D. W. Goodman, *Journal of Physical Chemistry*, 95 (1991) 5716-5719.
- [29] J. A. Rodriguez and D. W. Goodman, *Science*, 257 (1992) 897-903.
- [30] G. Liu, T. P. St Clair, and D. W. Goodman, *Journal of Physical Chemistry B*, 103 (1999) 8578-8582.
- [31] W. K. Kuhn, J. Szanyi, and D. W. Goodman, *Surface Science*, 303 (1994) 377-385.
- [32] W. K. Kuhn, J. W. He, and D. W. Goodman, *Journal of Vacuum Science & Technology A-Vacuum Surfaces and Films*, 10 (1992) 2477-2480.
- [33] P. J. Berlowitz and D. W. Goodman, *Langmuir*, 4 (1988) 1091-1095.
- [34] D. R. Rainer, J. S. Corneille, and D. W. Goodman, *Journal of Vacuum Science & Technology A-Vacuum Surfaces and Films*, 13 (1995) 1595-1599.
- [35] X. P. Xu and D. W. Goodman, *Journal of Physical Chemistry*, 97 (1993) 7711-7718.
- [36] J. Szanyi, X. P. Xu, and D. W. Goodman, *Abstracts of Papers of the American Chemical Society*, 206 (1993) 83-ETR.
- [37] X. P. Xu, J. Szanyi, Q. Xu, and D. W. Goodman, *Catalysis Today*, 21 (1994) 57-69.
- [38] X. P. Xu and D. W. Goodman, *Catalysis Letters*, 24 (1994) 31-35.
- [39] E. Ozensoy, B. K. Min, A. K. Santra and D. W. Goodman. submitted. 2003.
- [40] B. K. Min, A. K. Santra, and D. W. Goodman. *Applied Catalysis*, in press. 2003.
- [41] B. K. Min, A. K. Santra, and D. W. Goodman. *J. Vacuum Sci. & Technol. A*, in press. 2003.
- [42] D. R. Rainer, M. C. Wu, D. I. Mahon, and D. W. Goodman, *Journal of Vacuum Science & Technology A-Vacuum Surfaces and Films*, 14 (1996) 1184-1188.
- [43] D. R. Rainer, C. Xu, P. M. Holmblad, and D. W. Goodman, *Journal of Vacuum Science & Technology A-Vacuum Surfaces and Films*, 15 (1997) 1653-1662.
- [44] D. R. Rainer, S. M. Vesecky, M. Koranne, W. S. Oh, and D. W. Goodman, *Journal of Catalysis*, 167 (1997) 234-241.
- [45] D. R. Rainer, M. Koranne, S. M. Vesecky, and D. W. Goodman, *Journal of Physical Chemistry B*, 101 (1997) 10769-10774.
- [46] P. M. Holmblad, D. R. Rainer, and D. W. Goodman, *Journal of Physical Chemistry B*, 101 (1997) 8883-8886.
- [47] Y. Q. Cai, A. M. Bradshaw, Q. Guo, and D. W. Goodman, *Surface Science*, 399 (1998) L357-L363.
- [48] C. Xu, X. Lai, G. W. Zajac, and D. W. Goodman, *Physical Review B*, 56 (1997) 13464-13482.
- [49] C. Xu, W. S. Oh, G. Liu, D. Y. Kim, and D. W. Goodman, *Journal of Vacuum Science & Technology A-Vacuum Surfaces and Films*, 15 (1997) 1261-1268.
- [50] X. Lai, T. P. St Clair, M. Valden, and D. W. Goodman, *Progress in Surface Science*, 59 (1998) 25-52.
- [51] C. Xu and D. W. Goodman, *Chemical Physics Letters*, 263 (1996) 13-18.
- [52] F. M. Hoffmann. *Surface Science Reports* 3, 107. 1983.
- [53] D. W. Goodman, *Surface Review and Letters*, 2 (1995) 9-24.
- [54] D. W. Goodman, *Chemical Reviews*, 95 (1995) 523-536.
- [55] E. Ozensoy, C. W. Yi, C. Hess, J. H. Wang, and D. W. Goodman. in preparation. 2003.
- [56] R. D. Ramsier, Q. Gao, H. N. Waltenburg, K. W. Lee, O. W. Nooij, L. Lefferts, and J. T. Yates, *Surface Science*, 320 (1994) 209-237.
- [57] R. D. Ramsier, Q. Gao, H. N. Waltenburg, and J. T. Yates, *Journal of Chemical Physics*, 100 (1994) 6837-6845.
- [58] M. Bertolo, K. Jacobi, S. Nettesheim, M. Wolf, and E. Hasselbrink, *Vacuum*, 41 (1990) 76-78.
- [59] M. Bertolo and K. Jacobi, *Surface Science*, 265 (1992) 12-30.
- [60] *Electron spectroscopy for surface analysis*, eds. H. Ibach and J.D.Carette et al. (Springer-Verlag, Berlin; New York, 1977)
- [61] G. A. Somorjai and K. R. McCrea, *Advances in Catalysis*, Vol 45, 45 (2000) 385-438.
- [62] *Vibrational spectroscopy of molecules on surfaces*, eds. J. T. Yates (Plenum Press, New York, 1987)

- [63] T. Giessel, O. Schaff, C. J. Hirschmugl, V. Fernandez, K. M. Schindler, A. Theobald, S. Bao, R. Lindsay, W. Berndt, A. M. Bradshaw, C. Baddeley, A. F. Lee, R. M. Lambert, and D. P. Woodruff, *Surface Science*, 406 (1998) 90-102.
- [64] V. V. Kaichev, I. P. Prosvirin, V. I. Bukhtiyarov, H. Unterhalt, G. Rupprechter, and H. J. Freund, *Journal of Physical Chemistry B*, 107 (2003) 3522-3527.
- [65] M. K. Rose, T. Mitsui, J. Dunphy, A. Borg, D. F. Ogletree, M. Salmeron, and P. Sautet, *Surface Science*, 512 (2002) 48-60.
- [66] G. Rupprechter, *Physical Chemistry Chemical Physics*, 3 (2001) 4621-4632.
- [67] G. Rupprechter, H. Unterhalt, M. Morkel, P. Galletto, L. J. Hu, and H. J. Freund, *Surface Science*, 502 (2002) 109-122.
- [68] S. G. Sugai, H. Watanabe, T. Kioka, H. Miki, and K. Kawasaki, *Surface Science*, 259 (1991) 109-115.
- [69] S. Surnev, M. Sock, M. G. Ramsey, F. P. Netzer, M. Wiklund, M. Borg, and J. N. Andersen, *Surface Science*, 470 (2000) 171-185.
- [70] G. Blyholder, *Journal of Physical Chemistry* 68 (1964) 2772
- [71] M. R. Albert, *Journal of Catalysis*, 195 (2000) 62-66.
- [72] M. Bertolo and K. Jacobi, *Surface Science*, 236 (1990) 143-150.
- [73] W. A. Brown and D. A. King, *Journal of Physical Chemistry B*, 104 (2000) 2578-2595.
- [74] Q. Gao, R. D. Ramsier, H. N. Waltenburg, and J. T. Yates, *Journal of the American Chemical Society*, 116 (1994) 3901-3903.
- [75] H. Conrad, G. Ertl, J. Kuppers, and E. E. Latta, *Surface Science*, 65 (1977) 235-244.
- [76] K. H. Hansen, Z. Slijivancanin, B. Hammer, E. Laegsgaard, F. Besenbacher, and I. Stensgaard, *Surface Science*, 496 (2002) 1-9.
- [77] T. E. Hoost, K. Otto, and K. A. Laframboise, *Journal of Catalysis*, 155 (1995) 303-311.
- [78] M. Ikai and K. Tanaka, *Journal of Chemical Physics*, 110 (1999) 7031-7036.
- [79] A. J. Jaworowski, R. Asmundsson, P. Uvdal, and A. Sandell, *Surface Science*, 501 (2002) 74-82.
- [80] V. Johaneck, S. Schaueremann, M. Laurin, J. Libuda, and H. J. Freund, *Angewandte Chemie-International Edition*, 42 (2003) 3035-3038.
- [81] C. Nyberg and P. Uvdal, *Surface Science*, 204 (1988) 517-529.
- [82] S. W. Jorgensen, N. D. S. Canning, and R. J. Madix, *Surface Science*, 179 (1987) 322-350.
- [83] A. S. Mamede, G. Leclercq, E. Payen, P. Granger, and J. Grimblot, *Journal of Molecular Structure*, 651 (2003) 353-364.
- [84] I. Nakamura, T. Fujitani, and H. Hamada, *Surface Science*, 514 (2002) 409-413.
- [85] L. Piccolo and C. R. Henry, *Surface Science*, 452 (2000) 198-206.
- [86] R. D. Ramsier, K. W. Lee, and J. T. Yates, *Surface Science*, 322 (1995) 243-255.
- [87] R. Raval, M. A. Harrison, S. Haq, and D. A. King, *Surface Science*, 294 (1993) 10-20.
- [88] Y. A. Aleksandrov, I. A. Vorozheikin, K. E. Ivanovskaya, and D. G. Ivanov, *Russian Journal of Physical Chemistry*, 77 (2003) 202-205.
- [89] K. Almusaiter and S. S. C. Chuang, *Journal of Catalysis*, 180 (1998) 161-170.
- [90] K. Almusaiter and S. S. C. Chuang, *Journal of Catalysis*, 184 (1999) 189-201.
- [91] M. Date, H. Okuyama, N. Takagi, M. Nishijima, and T. Aruga, *Surface Science*, 350 (1996) 79-90.
- [92] M. Date, H. Okuyama, N. Takagi, and T. Aruga, *Applied Surface Science*, 121 (1997) 571-574.
- [93] R. Di Monte, J. Kaspar, P. Fornasiero, M. Graziani, C. Paze, and G. Gubitosa, *Inorganica Chimica Acta*, 334 (2002) 318-326.
- [94] A. Elhamaoui, G. Bergeret, J. Massardier, M. Primet, and A. Renouprez, *Journal of Catalysis*, 148 (1994) 47-55.
- [95] G. R. Garda, R. M. Ferullo, and N. J. Castellani, *Surface Review and Letters*, 8 (2001) 641-651.
- [96] G. W. Graham, A. D. Logan, and M. Shelef, *Journal of Physical Chemistry*, 97 (1993) 5445-5446.
- [97] M. Hirsimaki, S. Suhonen, J. Pere, M. Valden, and M. Pessa, *Surface Science*, 404 (1998) 187-191.
- [98] A. S. Mamede, G. Leclercq, E. Payen, P. Granger, L. Gengembre, and J. Grimblot, *Surface and Interface Analysis*, 34 (2002) 105-111.
- [99] K. Nakao, H. Hayashi, H. Uetsuka, S. Ito, H. Onishi, K. Tomishige, and K. Kunimori, *Catalysis Letters*, 85 (2003) 213-216.
- [100] L. Piccolo and C. R. Henry, *Applied Surface Science*, 162 (2000) 670-678.
- [101] L. Piccolo and C. R. Henry, *Journal of Molecular Catalysis A-Chemical*, 167 (2001) 181-190.
- [102] G. Prevot, O. Meerson, L. Piccolo, and C. R. Henry, *Journal of Physics-Condensed Matter*, 14 (2002) 4251-4269.
- [103] G. Prevot and C. R. Henry, *Journal of Physical Chemistry B*, 106 (2002) 12191-12197.
- [104] M. Valden, J. Aaltonen, E. Kuusisto, M. Pessa, and C. J. Barnes, *Surface Science*, 309 (1994) 193-198.
- [105] M. J. Weaver, *Surface Science*, 437 (1999) 215-230.
- [106] D. T. Wickham, B. A. Banse, and B. E. Koel, *Surface Science*, 243 (1991) 83-95.
- [107] C. T. Williams, A. A. Tolia, H. Y. H. Chan, C. G. Takoudis, and M. J. Weaver, *Journal of Catalysis*, 163 (1996) 63-76.
- [108] A. S. Worz, K. Judai, S. Abbet, and U. Heiz, *Journal of the American Chemical Society*, 125 (2003) 7964-7970.
- [109] V. P. Zhdanov and B. Kasemo, *Catalysis Letters*, 81 (2002) 141-145.
- [110] B. Hammer and J. K. Nørskov, *Advances in Catalysis*, Vol 45, 45 (2000) 71-129.
- [111] B. Hammer, *Journal of Catalysis*, 199 (2001) 171-176.
- [112] B. Hammer, *Physical Review Letters*, 89 (2002) art-016102.
- [113] K. Honkala, P. Pirila, and K. Laasonen, *Physical Review Letters*, 86 (2001) 5942-5945.
- [114] K. Honkala, P. Pirila, and K. Laasonen, *Surface Science*, 489 (2001) 72-82.
- [115] M. P. Jigato, K. Somasundram, V. Termath, N. C. Handy, and D. A. King, *Surface Science*, 380 (1997) 83-90.
- [116] Z. P. Liu and P. Hu, *Journal of the American Chemical Society*, 125 (2003) 1958-1967.
- [117] D. Loffreda, D. Simon, and P. Sautet, *Chemical Physics Letters*, 291 (1998) 15-23.
- [118] D. Loffreda, D. Simon, and P. Sautet, *Journal of Chemical Physics*, 108 (1998) 6447-6457.
- [119] D. Loffreda, D. Simon, and P. Sautet, *Surface Science*, 425 (1999) 68-80.
- [120] D. Loffreda, F. Delbecq, D. Simon, and P. Sautet, *Journal of Chemical Physics*, 115 (2001) 8101-8111.
- [121] D. Loffreda, D. Simon, and P. Sautet, *Journal of Catalysis*, 213 (2003) 211-225.
- [122] M. C. Asensio, D. P. Woodruff, A. W. Robinson, K. M. Schindler, P. Gardner, D. Ricken, A. M. Bradshaw, J. C. Conesa, and A. R. Gonzalezlope, *Chemical Physics Letters*, 192 (1992) 259-264.
- [123] R. Raval, *Surface Science*, 333 (1995) 1-10.
- [124] M. Bertolo and K. Jacobi, *Surface Science*, 226 (1990) 207-220.
- [125] A. Eichler, *Surface Science*, 526 (2003) 332-340.

- [126] G. W. Smith and E. A. Carter, *Journal of Physical Chemistry*, 95 (1991) 2327-2339.
- [127] S. M. Vesecky. Ph.D.Thesis, Texas A&M University, College Station. 1996.
- [128] M. L. Unland, *Science*, 179 (1973) 567-569.
- [129] M. L. Unland, *Journal of Catalysis*, 31 (1973) 459-465.
- [130] N. Macleod and R. M. Lambert, *Chemical Communications*, (2003) 1300-1301.
- [131] D. C. Chambers, D. E. Angove, and N. W. Cant, *Journal of Catalysis*, 204 (2001) 11-22.
- [132] N. W. Cant, D. C. Chambers, and I. O. Y. Liu. *Applied Catalysis B-Environmental*, in press. 2003.
- [133] F. Solymosi and T. Bansagi, *Journal of Catalysis*, 202 (2001) 205-206.
- [134] H. Celio, K. Mudalige, P. Mills, and M. Trenary, *Surface Science*, 394 (1997) L168-L173.